HUMAN-ROBOT COLLABORATION IN MICROGRAVITY: THE OBJECT HANDOVER PROBLEM

Virtual Conference 19–23 October 2020

Adriana Fernandes[1], Rodrigo Ventura[1]

[1]Institute for Systems and Robotics, Instituto Superior Técnico, Av. Rovisco Pais 1, 1049-001 Lisboa, Portugal, E-mail: adrianafernandes@tecnico.ulisboa.pt

[2]Institute for Systems and Robotics, Instituto Superior Técnico, Av. Rovisco Pais 1, 1049-001 Lisboa, Portugal, E-mail: rodrigo.ventura@isr.tecnico.ulisboa.pt

ABSTRACT

Collaborative space robots are an emerging technology with high impact as robots facilitate servicing functions in collaboration with astronauts with higher precision during lengthy tasks, under tight operational schedules, with less risk and costs, making them more efficient and economically more viable. However, human-robot collaboration in space is still a challenge concerning key issues in human-robot interaction, including mobility and collaborative manipulation of objects on a microgravity environment. In this paper we formulate an algorithm that enables a free-flyer robot, equipped with a manipulator, to perform an object handover between a human and a free-flyer robot, in a microgravity environment. To validate and evaluate this algorithm, we present a systematic user study with the goal of understanding the subjective outcome effects of a rigid and compliant impedance robot behavior during the interaction. The results showed that the rigid behavior was overall more preferable and registered higher transfer success during the tasks.

1 INTRODUCTION

Collaborative space robotics comprises the development of autonomous robots that are able to operate in microgravity environments facilitating manipulation, assembling or servicing functions in collaboration with astronauts. One of the reasons why space robots became progressively more relevant is their potential to offload tasks from astronauts, and thus reduce the crew size in-orbit. Robots also operate with extreme high precision and repeatability, being crucial on a demanding and safety-critical environment such as space. Additionally, the space environment is inherently risky, due to, e.g., radiation and space debris, posing an ever-present danger to astronauts.

Many advances were made regarding collaborative space robotics challenges but, to the best of the authors knowledge, no prior work on the field of object handover between humans and robots in microgravity was found in the literature. This problem differs from the terrestrial one by the absence of any cue to the human caused by weight of the object being handed over. Nevertheless, it is important to state relevant research in terrestrial object handovers of the following three phases: approach, transfer and retraction. Regarding the approach phase, Cakmak in [13] showed that robot's postures with an extended arm were most frequently classified handing over and Koay in [9] concluded that the robot should approach the user from the front. Furthermore, Aleotti in [8] stated that robots should take into consideration how the human will grasp the object and thus robots should approach the user with the easiest part to grasp of the object. Regarding the transfer phase, Edsinger in [4] found that humans will pose an object in the robot's stationary hand regardless of the robot's hand pose. Regarding the communication intent, Strabala in [2] claims that special signals can be used when the human and robot share the meaning of these signals in a common ground. Concerning the decision of releasing or grasping an object, Edsinger in [4] monitored the velocity of the robot's end-effector. To achieve a dynamic handover, Kupcsik's studied a Cartesian impedance control approach [11] and Kumagai in [3] presented an implementation of a human-inspired handover controller on a robot with compliant under-actuated hands. Concerning the retraction phase, Strabala in [2] stated that after transferring the entire object load, often the receiver will retract, indirectly signalling the giver that the handover is complete.

The goal of the this paper is to formulate an algorithm that enables a free-flyer robot equipped with a manipulator to perform an object handover with a human on a successful, fluent, and dynamic manner in a microgravity environment. The proposed algorithm is based on a Finite State Machine (FSM) coordinating the behavior of the robot during the following handover phases: approach, transfer, and retraction. A standard impedance controller was designed and implemented for the transfer phase, in which the object is grasped simultaneously by the human and robot.

For the validation and evaluation of the algorithm, a systematic user study was conducted, using an user interaction interface that was developed, based on a virtual reality environment. This environment uses the open-source Astrobee simulation platform [1]. The virtual reality environment uses a Leap Motion device for tracking in real time a human hand. This environment was used on a systematic user study.

The present paper is structured as follows: The Handover Algorithm Formulation is described in Section 2, including the derivation of the impedance controller. Furthermore, the Implementation and Results are presented in Section 3, the User Study is shown in Section 4 and Section 5 includes concluding remarks with future work references.

2 HANDOVER ALGORITHM FORMULATION

The proposed algorithm comprises two levels of abstraction: a Finite State Machine (FSM) modeling the multiple handover phases, and a set of motion controllers, one for each phase.

2.1 Robot-to-Human Handover

A robot-to-human object handover task aims to achieve an object transfer from a robot to a human where the robot acts as the giver and the human as the receiver. In this manner, a sequence of states and transitions of the FSM proposed were selected as Fig. 1 displays in green. Initially and assuming that the intention to perform a handover has already been established, the first state involves the opening of the gripper, followed by the movement to the object location which is assumed to be known by the robot. Upon arrival, the object must be grasped. It is important to refer that no specific grasping algorithm was designed given that the object grasping field was considered a sub-problem out of the scope of this paper. The next states involves the robot's movement into the handover pre-assigned location. Moreover, the robot should approach the user from the front as this angle provides him/her the most visibility of the robot's motion [9]. Furthermore, the robot's arm should be extended [13]. With the aim of delivering the object in a dynamic and fluent manner, an impedance control-based approach must be activated. This approach implements a dynamic response between the environment acting on the robot's manipulator structure and its motion. This module is further analysed in section 2.3. The impedance control (IC) activation is followed by the state regarding the user signalling in which the robot should communicate to the user that it is ready to deliver the object [2]. Another relevant stage of the transfer phase is the robot's decision concerning the appropriate time of releasing the object. Following the work developed by Edsinger in [4], the robot's end-effector velocity was monitored. In this manner, if the end-effector velocity is higher then the defined threshold, α, and the robot is grasping the object, the user's receiving intention is detected and the robot will open the gripper. The retraction phase is the last phase of the handover sequence. If the object has been delivered, the robot must switch off the formulated impedance control and move away from the handover location.

2.2 Human-to-Robot Handover

In a human-to-robot object handover task, the robot is the receiver and the human performs the giver role. A sequence of transitions and states of the proposed FSM describes a human-to-robot handover and it is presented in Fig. 1 in blue. The approach phase is initiated without the object and it is assumed that the robot already acknowledges the intention of receiving an object. As in the previous task, the robot's arm should be extended in the approach phase [13]. Furthermore, the opened gripper during the approach stage emphasis that intention. Upon arrival to the handover location, the same IC approach used on the robot-to-human handover task must be activated and the robot must signal the user. Furthermore, the robot must detect that the object has been placed in its end-effector. The work developed by Edsinger in [4] was again taken into consideration. Upon closing its gripper, the robot must verify the object reception success. This can be done by checking the resulting grasp aperture: if it is positive and above a threshold, β, then the gripper is assumed to be wrapped around an object and the retraction phase initiates, otherwise the robot must re-open the gripper and signal the user, showing the acknowledgement of the a failed transfer. Lastly, in the retraction phase, the IC must be switched off and the robot must move away from the handover location.

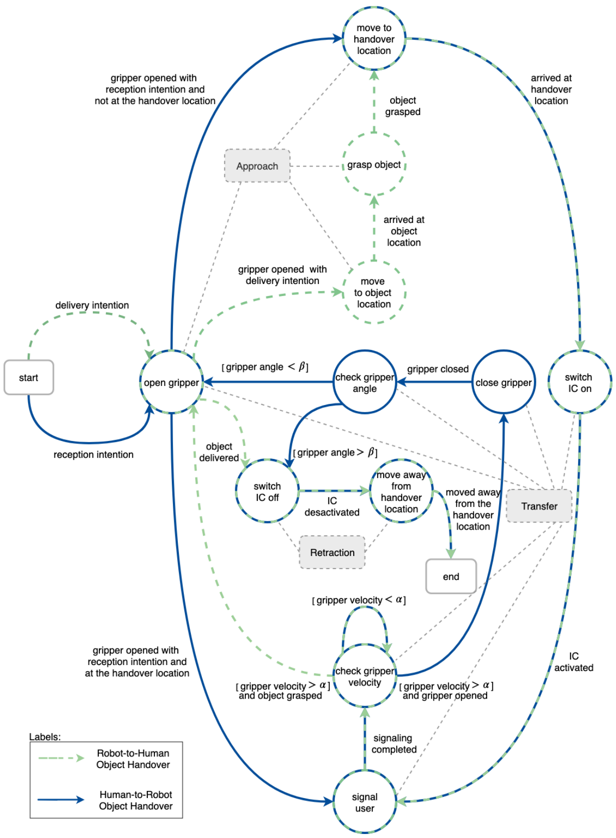

Figure 1: State-machine based algorithm sequence, in blue, regarding a human-to-robot handover. The three phases on the handover are also presented.

2.3 Impedance Control

A fluent and dynamic human-robot handover may be achieved due to the robot's adaptability to the task conditions, environmental constraints and perturbations instead of simply controlling its position, in which the robot is seen as an isolated system. As a result, impedance control was selected as the controlling approach for the transfer phase of the proposed FSM-based handover algorithm. This section aims to formulate an impedance controller that generates a dynamical relationship between a free-flyer robot manipulator and external forces acting on it. This formulation is adapted to this paper goals from the research developed by Lippiello and Ruggiero in [12].

2.3.1 Kinematic Model

The manipulator consists of n rigid links connected by joints q_l, with $l = 1, 2, 3, ..., n$. Moreover, the inertial frame is denoted by Υ_i, the body-fixed reference frame placed at the spacecraft center of mass by Υ_b and the end-effector coordinates attached to the interaction point of the manipulator by Υ_e. Furthermore, the absolute position of Υ_b with respect to Υ_i is described as $p_b^i = [x_b \; y_b \; z_b]^T$ and the system attitude is expressed in roll-pitch-yaw Euler angles being denoted by $\phi_b^i = [\varphi_b \; \theta_b \; \psi_b]^T$. Additionally, the absolute transitional velocity of Υ_b is represented by $\dot{p}_b^i$ and $\dot{p}_b^b$, with respect to Υ_i and to Υ_b, respectively. Regarding the absolute rotational velocity, ω_b^i refers to the absolute rotational velocity of the vehicle and ω_b^b denotes the absolute rotational velocity with respect to Υ_b. If the rotation matrix of frame Υ_b with respect to frame Υ_i is defined by R_b^i, the spacecraft linear velocity representation in Υ_b coordinates is transformed to its representation in Υ_i coordinates from:

$$\dot{p}_b^i = R_b^i \; \dot{p}_b^b \tag{1}$$

Moreover, if the transformation matrix between the time derivative of ϕ_b^i and ω_b^i is defined by N_b^i, the transformation of the free-flyer absolute rotational velocity is obtained as:

$$\omega_b^i = N_b^i \; \dot{\phi}_b^i \tag{2}$$

From (1) and (2) holds:

$$\omega_b^b = (R_b^i)^T \; \omega_b^i = (R_b^i)^T \; N_b^i \; \dot{\phi}_b^i = Q_b^i \; \dot{\phi}_b^i \tag{3}$$

with $Q_b^i = (R_b^i)^T \; N_b^i$ being the mapping of the time derivative of ϕ_b^i into the body absolute rotational velocity with respect to Υ_b. The transformation equations (1)-(3) are valid as long as the matrices R_b^i, N_b^i, and Q_b^i are non-singular. Furthermore, direct kinematics of the spacecraft are defined by the following transformation matrix:

$$K_b^i(p_b^i, \phi_b^i) = \begin{bmatrix} R_b^i(\phi_b^i) & p_b^i \\ 0_{1\times3} & 1 \end{bmatrix} \tag{4}$$

where, $0_{1\times3}$ is a (1×3) vector composed only by zeros. Furthermore, direct kinematics of the manipulator with respect to Υ_b are expressed as:

$$K_e^b(q) = \begin{bmatrix} R_e^b(q) & p_e^b(q) \\ 0_{1\times3} & 1 \end{bmatrix} \tag{5}$$

with q describing the $(n \times 1)$ vector of the robot manipulator joints variables, R_e^b the rotation matrix between Υ_e

and Υ_b and $p_e^b = [x_e^b \; y_e^b \; z_e^b]^T$ the position of the end-effector with respect to Υ_b. Combining (4) and (5):

$$K_b^i \; K_e^b = K_e^i(\xi) \tag{6}$$

where $\xi = [p_b^{i\,T} \;\; \phi_b^{i\,T} \;\; q_1 \;\ldots\; q_n]^T$ is the $((6+n) \times 1)$ generalized vector of the system joints variables. Moreover, the end-effector absolute position with respect to the inertial frame is defined as $x = [p_e^i \;\; \phi_e^i]$ where $p_e^i = [x_e \; y_e \; z_e]^T$ and the manipulator's attitude is also expressed in roll-pitch-yaw Euler angles being denoted by $\phi_e^i = [\varphi_e \; \theta_e \; \psi_e]^T$ with respect to Υ_i. The vector of absolute generalized velocity of the manipulator's end-effector can consequently be expressed as $\dot{x} = [\dot{p}_e^i \; \dot{\phi}_e^i]$. The transformation between $\dot{x}$ and the time derivative of the system generalized joints variables can be written as:

$$\dot{x} = J \, \dot{\xi} \tag{7}$$

where J is the so called Jacobian $(6 \times (6+n))$ matrix of the system. Moreover, time deriving (7) yields:

$$\ddot{x} = J \, \ddot{\xi} + \dot{J} \, \dot{\xi} \tag{8}$$

2.3.2 Dynamic Model

According to the *Euler-Lagrange* formulation, the Lagrangian of a mechanical system in the absense of gravity (and of any other source of potential energy) is simply given by $L = T$, where T is the total kinetic energy. The solution is given by the well-known Euler-Lagrange equation:

$$\frac{d}{dt}\frac{\partial L}{\partial \dot{\xi}_i} - \frac{\partial L}{\partial \xi_i} = u_i \tag{9}$$

with i describing the i-th generalized coordinate of ξ and assuming values of $i = 1, ..., ((6+n))$. The i-th generalized force is represented as u_i. The total kinetic energy of the system being studied is composed by the energy contributions concerning the motion of the spacecraft, T_b and the energy associated with motion of each link of the manipulator, T_{l_i}, as express in (10).

$$T = T_b + \sum_{i=1}^{n} T_{l_i} = \frac{1}{2} \, \dot{\xi}^T \; B \; \dot{\xi} \tag{10}$$

with B being an $((6+n)\times(6+n))$ symmetric and positive inertia matrix. Lastly, computing the Lagrange equation, the dynamics of the system in the generalized joint space are given by:

$$B(\xi) \; \ddot{\xi} + C(\xi, \dot{\xi}) \; \dot{\xi} = u + u_{ext} \tag{11}$$

where u describes the generalized input forces vector $((6+n) \times 1)$ and u_{ext} represents the external generalized forces vector at a joint level, $((6+n) \times 1)$. Furthermore, C is an $((6+n) \times (6+n))$ matrix that encompasses the Coriolis and centrifugal terms.

2.3.3 Control Law

Let $\ddot{x}_d$, $\dot{x}_d$ and x_d be the end-effector desired *rest* acceleration, velocity and position, respectively, and the actual position error as $\tilde{x} = x_d - x$. Moreover, during the transfer phase on the the handover tasks formulated it is assumed that $\ddot{x}_d = 0$ and $\dot{x}_d = 0$. Given these considerations, a suitable law control can be designed:

$$u = J^T \; (-K_B \; \dot{x} + K_D \; \tilde{x}) \tag{12}$$

With K_D and K_B representing the $((6+n)\times(6+n))$ symmetric and positive definite matrices of the chosen stiffness and damping, respectively. It is important to refer that these matrices can be tuned to the desired system's behavior. Finally, substituting (12) into (11) and considering (7) and (8), the joint space dynamics can be expressed in terms of the manipulator's end-effector configuration, x, in the inertial Cartesian coordinates representing an impedance dynamic model as presented in (13).

$$B_x \; \ddot{x} + (C_x + K_B) \; \dot{x} - K_D \; \tilde{x} = f_{ext} \tag{13}$$

with f_{ext} representing the vector $((6+n) \times 1)$ of the external generalized forces at the Cartesian coordinate level and B_x and C_x describing the inertia and Coriolis matrices with respect to the x variable:

$$B_x = J(\xi)^{-T} \; B(\xi) \; J(\xi)^{-1} \tag{14a}$$

$$C_x = J(\xi)^{-T} \; (C(\xi, \dot{\xi}) - B(\xi) \; J(\xi)^{-1} \; \dot{J}(\xi)) \; J(\xi)^{-1} \tag{14b}$$

with $^{-T}$ being the inverse of transpose.

Summarizing, a control law was designed for the transfer phase of the formulated FSM-based handover algorithm given the kinematics and dynamics of a microgravity free-flying robot equipped with a manipulator.

3 IMPLEMENTATION AND RESULTS

Given the availability of an open-source Astrobee software platform designed to conduct research [1], this free-flyer robot simulator was used as an implementation platform to showcase and verify the formulated handover algorithm. In the future, this formulation and implementation can validated on the Astrobee aboard the ISS. The implement was done using Python 3.0, Ubuntu 16.04 LTS and ROS Kinetic.

3.1 Impedance Control Validation

Regarding the impedance control module, it is important to refer that although an impedance control formulation for a free-flyer robot equipped with a manipulator was described on section 2.3, the Astrobee's Gazebo simulator[1] presented considerably small tolerances for the joints state goals. Thus, it does not allow the movement of the arm links for small controlled angles and the joint variables are assumed to be fixed for this implementation. In this manner:

$$\dot{\xi} = [\dot{p}_b^{i\,T} \; \dot{\phi}_b^{i\,T} \; 0 \; ... \; 0]^T \tag{15}$$

Moreover, two types of impedance behaviors were implemented: rigid and compliant. These behaviors can be defined by tuning the values of the matrices K_D and K_B in (12). In order to obtain the formulated impedance controller validation during interaction, several generalized external forces, f_{ext}, were applied to the robot's end-effector, for both behavior study cases. Furthermore, with the aim of validating the dynamic impedance model proposed, the expected values of the end-effector position and orientation error, $\tilde{x}'$, were computed from (13) given the end-effector simulated acceleration, $\ddot{x}$, the end-effector simulated velocity, $\dot{x}$, the B_x, C_x, K_D and K_B matrices and the f_{ext}, as follows:

$$\tilde{x}' = K_D^{-1} \; [B_x \, \ddot{x} + (C_x + K_B) \, \dot{x} \; - f_{ext}] \tag{16}$$

The end-effector position and orientation errors, $\tilde{x}'$, as well as the actual simulated end-effector position and orientation error, $\tilde{x}$, are presented each axis in Fig. 2 for the rigid behavior and for the compliant behavior case. Additionally, the external generalized forces generated for each simulation are represented.

Analysing the presented figures, several conclusions can be drawn. The first one concerns the clear motion distinction between the two behaviors: a higher stiffness value in (13) generates a rigid behavior where the end-effector tends to reach the desired state with a lower position/orientation error and a lower stiffness value generates robot's motion passively to the external perturbation, diverging more from the desired state. Furthermore, the robot not only reaches for desired/rest state for both behaviors while an external force acts on the end-effector, but also in the absence of external perturbations. Lastly, the end-effector behaves accordingly to desired impedance model expressed by (13). This can be concluded due to the overlap of the actual simulated end-effector error motion, $\tilde{x}$, and the computer end-effector error motion from the impedance model, $\tilde{x}'$.

[1] https://www.nasa.gov/astrobee

3.2 Human Interaction Implementation

The algorithm proposed assumes that two agents are involved in the handover: a robot and a human. Thus, a simulated hand model controlled via a real user hand was implemented. The main requirement concerning the simulated hand model is its the ability to mimic a human hand in terms of its degrees of freedom. The iCub robot hand ended up being selected and integrated into the Gazebo simulation, as no other more photo realistic simulated human hand was found by the authors. To control the simulated hand, the values of the real user hand position/orientation and fingers were tracked via a Leap Motion device and integrated on the interface. Fig. 3 displays the user hand, the Leap Motion device and the simulation environment.

It should be acknowledge that the absense of any haptic feedback on the user hand is a limitation of this study. Thus, the visual feedback of the virtual environment is the only modality the user has to perceive the environment state.

3.3 Handover Algorithm Validation

The algorithm was validated in both proposed tasks. In the case of a robot-to-human handover and as formulated, the robot initiated the handover with a closed gripper and without the object. It then opened the gripper, got closer to the object and grabbed it. Following, the robot moved to the handover location. After activating the IC, the robot was ready to deliver the object and the Transfer phase initiated in which the Astrobee signaled the user using its flashlight and waited for the gripper velocity threshold. When this occurs, the robot opened its gripper and the object is transferred to the user. Lastly, both moved away from the handover location. In the case of a human-to-robot handover, the robot initiated the handover with a closed gripper and without the object as the user is grabbing it. It then opened the gripper and moved to the same handover location. After activating the IC, the robot was ready to receive the object and thus, the Transfer phase initiated in which the robot signaled the user and waited to detect the object placement on its end-effector. When this occurs, the transfer of the object was performed and

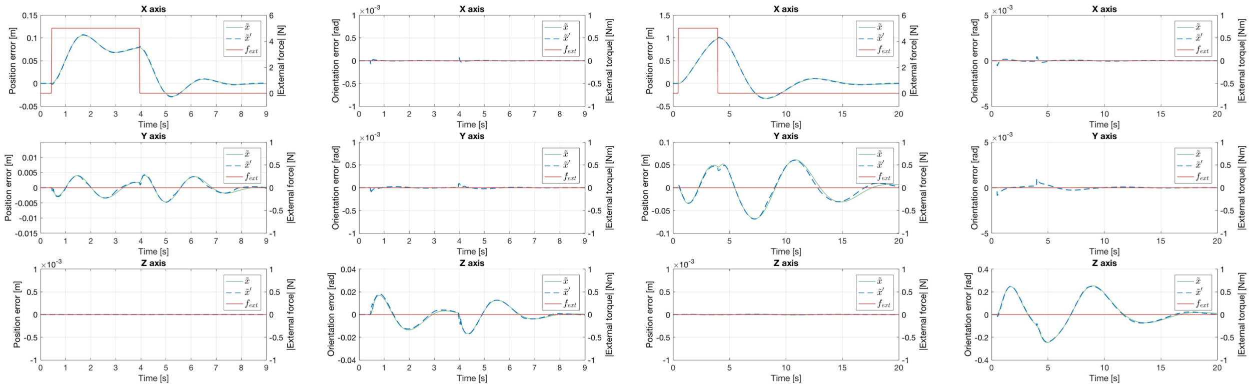

Figure 2: Actual and computed (from impedance model) end-effector position and orientation error, with a rigid behavior (6 figures on the left) and compliant behavior (6 figures on the right). A $5N$ force was applied on the X axis.

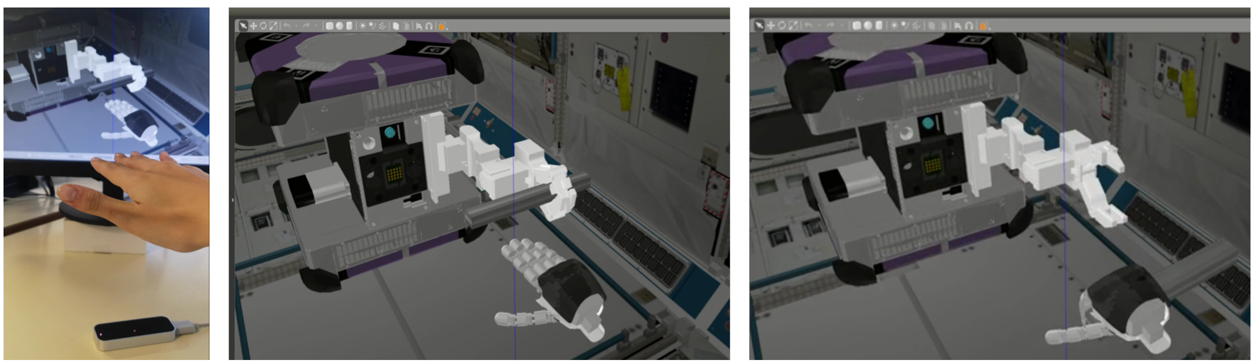

Figure 3: Virtual reality simulation environment. Left: human hand being tracked by the Leap Motion device (bottom), and the simulated hand on the computer screen. Center and right: Astrobee simulation environment showing the robot handing over a cylindrical bar to the simulated hand.

the user hand model and the Astrobee moved away from the handover position. Furthermore, the failure detection module was successfully validated given that the robot acknowledge a test failed transfer by re-opening the gripper and re-signaling the user. Lastly, during the transfer for both tasks the gripper motion was in accordance to the impedance control results, given that, for a similar user external interaction, the gripper's movement was minimum for a rigid behavior and it moved passively to simulated user hand for the compliant case.

4 USER STUDY

Based on the results of Kupcsik's study [11] it is known that for static handover tasks using cartesian compliant control, compliance parameters are less important for success and high stiffness is always preferred and highly rated. Gasparri in [5] shows that when using impedance handover dynamics the optimal manipulator stiffness is high in the case of perfect knowledge of the framework. In this sense, the systematic user study aimed to explore the subjective outcomes effects on the user concerning the implemented robot behaviors. Furthermore, the handover success of the two behaviors was also studied. In this sense, two hypothesis were in advance proposed for the experimental study:

H1: *The impedance control parameters will affect the participant's perception of the object handover task with high stiffness (rigid behavior) being the most fluent, desirable and cooperative and low stiffness (compliant behavior) the less fluent, desirable and cooperative;*

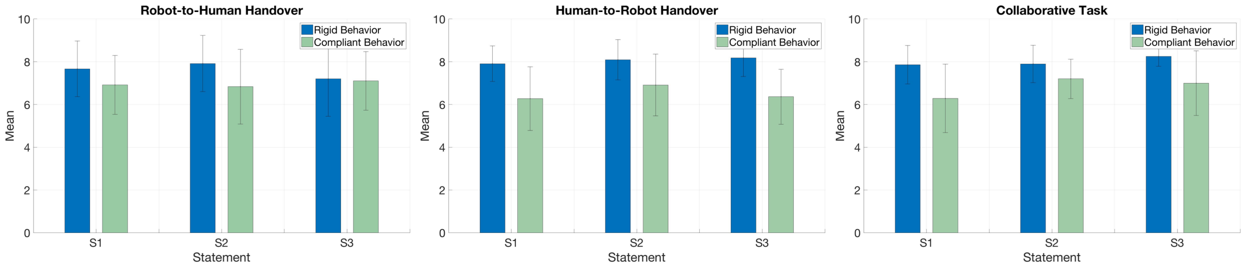

Figure 4: Representation of the mean and standard deviation of the questionnaire's results for the performed tasks.

H2: *the impedance control parameters will affect the object handover task success with high stiffness (rigid behavior) being the most successful and low stiffness (compliant behavior) the less successful.*

Ten people with ages between 21 and 30 participated in this experiment (6 female and 4 male). Initially each participant performed different manoeuvres of their choice with the simulated hand for 10 minutes. The second section of the experiment was the handover tasks: robot-human, human-robot handover and a collaborative task that encompassed both handovers. Moreover, the controller parameters conditions were adjusted in order to achieve rigid behavior or compliant behavior. The study involved 12 rounds of interaction for each participant – two for each experimental condition with randomized controlled trials. After each round of interaction, participants filled out a questionnaire giving a score between 1 (fully disagree) and 9 (fully agree) [10] to three statements regarding their perception of the handover. In particular three scales were used — fluency [6] and [7], satisfaction [10] and team work [6]. The statements were the following:

S1: "The robot contributed for the fluency of the interaction.";

S2: "I was satisfied with the interaction.";

S3: "The robot was committed to the task."

Additionally, the number of non-successful object handover in the three tasks were registered.

4.1 Results

The questionnaire's results are presented in Fig. 4, for the proposed tasks. Additionally, Table 1 displays the total number of failed transfers for each task.

Table 1: Total number of failed handovers from a total of 12 runs, on the three performed tasks.

		Rigid Behavior	Compliant Behavior
Task	Robot-to-Human Handover	3	3
	Human-to-Robot Handover	0	2
	Collaborative	2	3

Concerning the user's responses to the proposed statements, the results indicate that in a robot-to-human handover scenario users tended to perceive higher fluency for a rigid behavior (p-value $= 0.1195$) and tended to be more satisfied with the interaction also for the rigid behavior (p-value $= 0.0589$). Moreover, no substantial difference between both behaviors was felt regarding the robot commitment to the task (p-value $= 0.8880$) and thus concerning the cooperation perceived. Additionally, results shows higher distinction between the answers regarding the two behaviors in the human-to-robot handover scenario, as users perceived more fluency, satisfaction and cooperation for a rigid behavior, with statistical significance (p-value of 0.0132, 0.0401 and 0.0057, respectively). As expected, for the collaborative task, the results were also higher for the rigid behavior concerning S1, S2 and S3, with statistical significance (p-value of 0.0375, 0.0445, 0.0492, respectively). Lastly, more total successful handovers were performed for the rigid behavior. Summarizing, the results indicate that H1 was verified for the first two factors and the handover success data supported H2 for the human-to-robot object handover and collaborative task. In this sense, the users perceived an overall more fluent, dynamic and successful object handover for the rigid behavior.

5 CONCLUSIONS AND FUTURE WORK

This paper formulated and validated an algorithm enabling a free-flyer robot to perform an object handover with a human in a microgravity environment, in a dynamic, fluent and successful manner, combining a FSM and an impedance controller. Furthermore, a virtual reality user interaction interface on a realistic robotic simulator was developed and a systematic user study was conducted where results showed that the rigid behavior was overall more preferable and registered higher transfer success during the proposed tasks. Future work may address the integration of a grasping algorithm, the extension to include motion of the robot arm during the handover, and the extension to multiple robots for handovers tasks with large objects. Concerning validation, future work may include integrating haptic feedback in the interface, in order to provide tactile feedback of the handover task, as well as performing test sessions on the ISS using the real NASA Astrobee robots.

Acknowledgement

This work was supported by the FCT Project LaRSYS (UIDB/50009/2020) and the ANI P2020 project INFANTE (10/SI/2016).

References

[1] L. Fluckiger, K. Browne, B. Coltin, J. Fusco, T. Morse and A. Symington, Astrobee Robot Software: Enabling Mobile Autonomy on the ISS, in Proc. of the Int. Symposium on Artificial Intelligence, Robotics and Automation in Space (i-SAIRAS), 2018

[2] K. W. Strabala, M. K. Lee, A. D. Dragan, J. L. Forlizzi, S. Srinivasa, M. Cakmak and V. Micelli, Towards Seamless Human-Robot Handovers, Human–Robot Interaction, vol. 2, no. 1, pp. 112-132, 2013

[3] W. P. Chan, I. Kumagai, S. Nozawa, Y. Kakiuchi, K. Okada and M. Inaba, Implementation of a robot-human object handover controller on a compliant underactuated hand using joint position error measurements for grip force and load force estimations, IEEE International Conference on Robotics and Automation (ICRA), 2014

[4] A. Edsinger and C. C. Kemp, Human-Robot Interaction for Cooperative Manipulation: Handing Objects to One Another, The 16th IEEE International Symposium on Robot and Human Interactive Communication (RO-MAN), 2007

[5] G. M. Gasparri, F. Fabiani, M. Garabini, L. Pallottino, M. Catalano, G. Grioli, R. Persichin and A. Bicchi, Robust optimization of system compliance for physical interaction in uncertain scenarios, IEEE-RAS 16th International Conference on Humanoid Robots, 2016

[6] G. Hoffman, Evaluating fluency in human-robot collaboration, IEEE Transactions on Human-Machine Systems, vol. 49, no. 3, pp. 209-218, June 2019.

[7] C. M. Huang, M. Cakmak and B. Mutlu, Adaptive Coordination Strategies for Human-Robot Handovers, Robotics: Science and Systems XI (RSS), 2015.

[8] J. Aleotti, V. Micelli and S. Caselli, Comfortable robot to human object hand-over, Robot and Human Interactive Communication (RO-MAN), pp. 771-776, 2012

[9] K. Koay, E. Sisbot and D. Syrdal, Exploratory studies of a robot approaching a person in the context of handing over an object, AAAI Spring Symposium: Multidisciplinary Collaboration for Socially Assistive Robotics, pp. 18-24, 2007

[10] M. Koene, S. Endo, A. Remazeilles, M. Prada and A. M. Wing, Experimental testing of the CogLaboration prototype system for fluent Human-Robot object handover interactions, The 23rd IEEE International Symposium on Robot and Human Interactive Communication (RO-MAN), 2014.

[11] A. Kupcsik, D. Hsu and W. S. Lee, Learning Dynamic Robot-to-Human Object Handover from Human Feedback, Springer Proc. in Advanced Robotics Robotics Research, pp. 161-176, 2017.

[12] V. Lippiello and F. Ruggiero, Cartesian Impedance Control of a UAV with a Robotic Arm, IFAC Proc. Volumes, vol. 45, no. 22, pp. 704-709, 2012.

[13] M. Cakmak, S. S. Srinivasa, M. K. Lee, S. Kiesler and J. Forlizzi, Using Spatial and Temporal Contrast for Fluent Robot-Human Hand-overs, International Conference on Human-Robot Interaction (HRI), pp. 489-496, 2011.